The Role of Cell Wall Mutation in the Pathogenicity of *E. coli* H7:O157: A Molecular Evolution Study

Walaa A. Sallomi , Rebah N. Algafari * , Ikram Abbas Abbood

Posted Date: 13 October 2025

doi: 10.20944/preprints202510.0833.v1

Keywords: *E. coli* H7:O157; microbial pathogenesis; bacterial cell wall modification; site-directed mutagenesis

 doi:10.20944/preprints202510.0833.v1

Article

The Role of Cell Wall Mutation in the Pathogenicity of *E. coli* H7:O157: A Molecular Evolution Study

Short title: Cell Wall-Associated Pathogenesis in *E. coli*

Walaa A. Salloomi [1], Rebah N. Algafari [2,*] and Ikram Abbas Abbood [1]

[1] Baghdad University, College of Veterinary Medicine, Department of Microbiology

[2] Al-Nahrain University, Biotechnology Research Center, Department of Environmental Biotechnology

* Correspondence: rabahalgafari@nahrainuniv.edu.iq

Abstract

E. coli H7:O157, the causative pathogen of many disease outbreaks and cases of food poisoning, has been the subject of many studies. The bacterium's pathogenicity is highly associated with cell wall modifications and changes. A total of 20 fecal samples from patients who showed the typical symptoms of the infection tested positive for *E. coli* H7:O157 and another 20 samples from animals were also collected. The bacterium was isolated and identified using cultural and molecular methods. The *waa* K, *waa* L, and *waa* Y sites were subjected to site-directed mutagenesis, and the effect of these mutations were studied and analyzed through its influence on the pathogenicity compared to the wild type. We found that the invasiveness and morbidity of mutant *E. coli* H7:O157 increased significantly when ingested by laboratory animals. This may be attributed to *waa* K and *waa* L, since they led to a significant change in the transmembrane helix ratio compared to the wild type, enabling the uncontrolled release of the Shiga toxin into the infected animals, causing their death in 6 hours. Specific sites in the *waa* operon, namely *waa* K and *waa* L, play the leading role in controlling the progress of pathogenicity. Mutations in these sites may increase the virulence of this bacterium.

Keywords: *E. coli* H7:O157; microbial pathogenesis; bacterial cell wall modification; site-directed mutagenesis

1. Introduction

The Shiga toxin-producing *E. coli* O157:H7 (STEC) was identified in 1982 as a human pathogen [1]. *E. coli* O157:H7 was thus named due to its ability to express the somatic (O) antigen with flagellar antigen (H) [7]. MacConkey agar supplemented with MUG and sorbitol was used to identify and select the original isolate of *E. coli* O157:H7 [15]. STEC is a zoonotic pathogen causing worldwide outbreaks [2] with the virulence factors Shiga toxins 1 and 2 [3]. Additional virulence factors have been identified represented by plasmid-encoded enterohemolysin (EhxaA), autoagglutination adhesion (Saa), a catalase-peroxidase (KatP), and others [4]. This strain is also known as enterohemorrhagic *E. coli* (EHEC) and can cause hemorrhagic colitis (HC), which can be life-threatening, with sequelae including hemolytic uremic syndrome (HUS) [5]. The bacterium has also been isolated from animals (farm livestock). The spread of such an infection may lead to a decline in animal production, especially in the case of poultry and large animals, due to abdominal sepsis, urinary tract infections, blood poisoning, and diarrhea [6].

E. coli O157:H7 is transmitted through food, such as dairy products and vegetables that are contaminated with the feces of infected animals [7,8]. Large animals like sheep and cattle are the fundamental reservoirs of *E. coli* O157:H7 [9,10]. Pets like birds and dogs can be considered a secondary route of infection [11].

Intestinal colonization by *E. coli* O157:H7 is accompanied by damage to the lining cells due to the production of Shiga toxin [12]. The bacterium can resist the host's defense mechanism and mimics

 doi:10.20944/preprints202510.0833.v1

part of the normal intestinal flora [13]. Adhesion to intestinal epithelial cells is considered the first step in STEC interactions, and the binding patterns of STEC and epithelial cells are unique to *eae*-negative STEC strains. Many EHEC are *eae*-positive, and the *eae* gene is considered a risk factor for HUS [14].

The genome size of *E. coli* O157:H7 is 5.5 Mb with a 4.1 Mb backbone sequence conserved in *E. coli* strains [16]. When the genome size of *E. coli* O157:H7 was compared with that of non-pathogenic *E. coli*, there was about 0.53 Mb missing in the former, suggesting that an evolutionary mechanism played a role in the development of this strain [17,18].

Antibiotic resistance is one of the characteristics of *E. coli* O157:H7 that increases its pathogenicity. It has been found to be highly resistant to quinolones, aminoglycosides, macrolides, and others [19]. In addition to the occurrence of *E. coli* O157:H7, the spread of other antimicrobial-resistant bacteria and multidrug-resistant zoonotic foodborne pathogens has become a worldwide problem [20]. Resistance genes are the main factor behind antibiotic resistance, but the cell wall and the shape transition of the cell may also play critical roles in this mechanism [21,22]. Some studies [23,24] have dealt with chemical modifications, the destruction of antibiotics, or changes in cell wall structure that inhibit antibiotic action, but the molecular underpinnings of such changes need to be addressed and clarified, which is what led to this study. This study aimed to determine the tendency of the bacterium cell mutation, consequence of this mutation on the bacterium, and its effect on the pathogenecity and ability to infect the target host.

2. Materials and Methods

2.1. Ethics and Participation in This Study

2.1.1. Animal Welfare and IRB Approval

The Biotechnology Research Center's IRB at Al-Nahrain University issued ethical approval for experiments potentially impacting animal welfare with reference no. PG/244, following EU Directive 2010/63/EU.

2.1.2. Human Sample Collection Approval

The Biotechnology Research Center at Al-Nahrain University approved human sample collection after patients gave written consent—an ethical approval document with the reference no. C.B 242 was issued for this purpose.

2.1.3. Sample Collection

A total of 40 fecal samples and watery intestinal exudates released by human patients admitted to Al-Yarmouk Teaching Hospital or Al-Kindy Teaching Hospital were collected. The samples were immediately processed at the clinical laboratories of the hospitals by cultivation in nutrient broth and then they were transferred after 24 hours to the university's laboratories for further processing.

Furthermore, 40 animal feces samples were collected from large animals such as cows and sheep showing symptoms of diarrhea, cold extremities, unsteadiness, and difficulty standing. The samples were preserved in a transport medium and transferred to the university's laboratories using a cool box. Upon arrival, these samples were diluted with sterile normal saline and cultured in nutrient broth for 24 hours to enable bacterial growth.

2.1.4. Isolation of E. coli O157:H7

Samples enriched in nutrient broth were diluted to 10^6 and cultivated on MacConkey agar (Oxoid, U.K.) for 24 hours at 37^0 C. Colorless colonies were transferred and spread on Eosin Methylene Blue agar (EMB) (Hi Media, India) and allowed to grow for 24 hours at 37^0 °C. *E. coli* colonies that showed a metallic sheen were selected and cultivated on Hi Chrome medium with

 doi:10.20944/preprints202510.0833.v1

supplements (Hi Media, India) for 24 hours at 37^{0}C. Colonies of *E. coli* O157:H7 exhibited a dark purple to magenta color.

2.2. Molecular Identification of E. coli O157:H7

2.2.1. Extraction of DNA from Bacterial Cells

DNA was extracted from the cultivated colonies obtained from samples culturing using the GenX total DNA extraction kit (UK) according to the manufacturer's instructions. About 105 µg of DNA was obtained on average from each bacterial sample, with a purity of 1.8, as measured by the NanoDrop system (Techne, UK). DNA samples were preserved at -20^0 °C until processing.

2.2.2. PCR Amplification of Specific *E. coli* O157:H7 Genes

E. coli O157:H7 possesses a unique set of genes by which it can be easily identified. Genes that were detected in the isolate under study were as follows:

2.2.3. The *rpo*B gene

The *rpo*B gene was amplified using specific primers designed for this purpose using the gene sequence deposited within the NCBI database under accession no. JX471606. The sequences of the primers are rpF 5′ CAGCCAGCTGTCTCAGTTTAT 3′ and rpR 5′ GGCAAGTTACCAGGTCTTCTAC 3′. The Thermocycler (LabNet, USA) program was one cycle of denaturation at 95^0 °C for 2 min, followed by 35 cycles of denaturation at 94^0 °C for 30 sec, annealing at 49^0 °C for 30 sec, and extension at 72^0 °C for 30 sec. After the 35 cycles, the samples were subjected to a final extension at 72^{0}C for 10 min, and held at 4^0 °C until they were removed from the thermocycler. The amplicons obtained were preserved at -20^0 °C.

2.2.4. The *waa* Gene

This site was amplified with the specific primers designed for this purpose based on the gene sequence with the accession no. M95398 in the NCBI database. The primer sequences were as follows: waa F 5′ CACTAATTTTACGTGGCAGAC 3′ and waa R 5′ CCCATATGATCACATCAACTGA 3′. The thermocycler program was one cycle of denaturation at 95^0 °C for 2 min, followed by 35 cycles of denaturation at 94^0 °C for 30 sec, annealing at 59^0 °C for 30 sec, and extension at 72^0 °C for 30 sec. When the samples were completely amplified, they were subjected to final extension at 72^{0}C for 10 min, and held at 4^0 °C.

2.2.5. The Shiga Toxin Stx Gene

The following primers were designed to amplify *the stx* 1 gene based on the accession number OM304351 in the NCBI database. The primer sequences were stxF 5′ CAGTTAATGTCGTGGCGAAGG 3′ and stxR 5′ CACCAGACAATGTAACCGCTG 3′. The gene was amplified using the following program: 95^{0}C (1 cycle), denaturation at 94^{0}C for 30 sec, annealing at 55^{0}C, and extension at 72^{0}C (35 cycles). Final extension was conducted at 72^{0}C for 10 min, and the samples were held at 4^{0}C.

2.2.6. The *rfbO* Gene

The *rfb*O was targeted for amplification by PCR using specific primers designed for this purpose based on the accession no. X59852 from the NCBI. The primers' sequences were rfoF 5 ′CGTGATGATGTTGAGTTG 3′ and rfoR 5′ AGATTGGTTGGCATTACTG 3′. PCR amplification of the target gene was performed under the following conditions: one cycle of initial denaturation at 95 °C for 2 min, followed by 35 cycles of denaturation at 94 °C for 30 sec, annealing at 59 °C for 30 sec, and extension at 72 °C for 30 sec. The final extension followed at 72^0 C for 10 min, and the samples were held at 4^{0}C until they were removed from the thermocycler.

 doi:10.20944/preprints202510.0833.v1

Primer used for site-directed mutagenesis and cloning experiment.

The cell wall-controlling operon *waa* was targeted for mutagenesis. A primer was designed for these purposes using the software available at https://nebasechanger.neb.com. The primer used for site-directed mutagenesis, after adding the sticky ends complementary to the cloning vector, is highlighted in gray. The primer sequence was mutCF 5′ T CAG CAA GGG CTG AGGcgcacatcctttaaacttcattcattg 3′ and mutCR 5′ catttaattaattgtattgttacgattattaatgG GGA GTC GAA GGC GACT 3′. The PCR program was initial denaturation at 95^0 °C for 2 min (1 cycle), followed by 30 cycles of denaturation at 94^0 °C, annealing at 63 °C for 1 min, and extension at 72 °C for 1 min. The final extension was performed at 72 °C for 10 min, and the samples were held at 4^0 C after the reaction was completed.

2.2.7. Site-Directed Mutagenesis

The PCR product of the *waa* gene was used as a template for the mutagenesis experiment. An amount of 2 µl of PCR *waa* amplicon was mixed with 1 µl of mutCF and 1 µl of mutCR (the final concentration was 0.5 pmol of each primer) in a master mix tube (Bioneer, Korea) and subjected to PCR amplification according to the following program: initial denaturation at 95^0 C for 2 min (1 cycle), followed by 30 cycles of denaturation at 94^0 C, annealing at 62^0 C for 1 min, and extension at 72^0 C for 1 min. The final extension was performed at 72 °C for 10 min, and the samples were held at 4 °C after the reaction was completed.

2.2.8. Cloning of the Mutated *waa* Gene

Cloning of the mutated *waa* gene was performed using the MB324 NZYEasy Cloning & Expression kit (NZYTech, Portugal).

2.2.9. Transformation Procedure

The transformation procedure was performed for both competent cells (NZYTech DL3 star *E. coli*) and the wild type. The transformation protocol was achieved with the following steps: A volume of 10 µl of ligation product obtained from the cloning experiment was mixed directly with 100 µl of recipient cells and placed on ice for 30 min. The mixture was removed and subjected to heat shock at 42 °C for 40 seconds and placed on ice again for 2 minutes. A pre-warmed SOC medium was added to the cells and incubated at 200 rpm at 37^0 C for 1 hour. The cells were then precipitated by centrifugation at 5000 rpm for 1 min, and the remaining medium was removed. After the precipitation step, the cells were gently re-suspended by pipetting, and 100 µl of the cells was spread on LB agar plates with 50 µg/ml kanamycin. The plates were incubated at 37 °C overnight to allow only the transformant to grow.

The same protocol was used to transform wild-type *E. coli* with one modification. This modification was treating the cells with lysozyme (10 µg/ml) for 1 hour at 4^0C before proceeding to the transformation protocol.

2.2.10. Confirmation of Cloning and Transformation

Electrophoresis confirmed cloning of the mutated gene. An amount of 2 µl of standard mixture (pHTP9) only and the cloned product (pHTP9 with mutated gene) were subjected to PCR amplification using the mutCF, and mutCR primers, and the pHF 5′ GAATGAAAAACGCGACCACATGGTG 3′ and pHR 5′ GGTTATGCTAGTTATTGCTCAGCG 3′ primers were designed by the NZYTech Company to specifically detect the pHTP9 vector. The difference in DNA bands resolved by electrophoresis differentiates between the standard cloning product and the one with a mutated gene. Colony PCR was performed to confirm successful cloning and transformation.

2.2.11. Sequencing of PCR Products

 doi:10.20944/preprints202510.0833.v1

PCR products were sent to Macrogen Corp. (Korea) for sequencing by the Sanger method.

2.2.12. Animal Experiment

The experiment was performed with 180 BALB/c mice, which were divided into 3 groups. Each group contained 60 mice that were further subdivided into groups of 30 mice, except for the third group which contained the control mice, resulting in a total of five groups named and treated as follows: group 1-1 was infected with wild-type *E. coli* O157:H7 without treatment; group 1-2 was infected with wild-type *E. coli* O157:H7 and treated with cefotaxime; group 2-1 was infected with mutated *E. coli* O157:H7 and left without treatment; and finally group 2-2 was infected with mutated *E. coli* O157:H7 and also treated with cefotaxime. The third group, which was composed of the control mice, was kept away from the other groups to prevent the infection with the pathogen. Blood was drawn from groups 1 and 2 when they showed symptoms of infection as identified by a professional veterinarian, and both the liver and kidney function were measured in order to be compared with mice in the same group and with other groups.

2.2.13. Data Analysis and Bioinformatics

Sequences obtained by PCR amplification were analyzed using available tools on the NCBI website (https://www.ncbi.nlm.nih.gov), including BankIt (https://submit.ncbi.nlm.nih.gov/about/bankit/), BLASTN (https://blast.ncbi.nlm.nih.gov/Blast.cgi?PROGRAM=blastn&PAGE_TYPE=BlastSearch&LINK_LOC=blasthome), BLASTX (https://blast.ncbi.nlm.nih.gov/Blast.cgi?PROGRAM=blastx&PAGE_TYPE=BlastSearch&LINK_LOC=blasthome), and Phyre2, which is available at http://www.sbg.bio.ic.ac.uk/phyre2/html/page.cgi?id=index.

2.2.14. Statistical Analysis

The Statistical Packages of Social Sciences (SPSS 2018) was used for statistical analysis. The parameters measured during the study were input to calculate the least significant difference (LSD) in order to evaluate the statistical significance of the differences among the tested groups.

3. Results

3.1. Isolation of E. coli O157:H7 and Morphological Characteristics

Among all of the samples from humans and animals, only 20 from each were positive for *E. coli*. The isolation and identification of the bacterium was performed by culture media before using molecular methods. Colonies with a mauve color, which is a characteristic of *E. coli* O157:H7, were selected to continue this study. Figure 1 in the Supplementary Materials shows the growth of *E. coli* O157:H7 on different media.

3.2. Molecular Identification and Classification of E. coli O157:H7

During this study, we used the *rpoB* gene to identify and classify the bacterium under study. The gene was amplified, sequenced, and the BLAST tool was used for its identification. The results of PCR amplicons sequencing showed that it belongs to the *E. coli* O157:H7 strain Sakai, and our sequence was deposited in the NCBI database under accession no. PP059841. Figure 2 shows the electrophoresis results of the *rpoB* gene amplified from isolates from humans and animals (Supplementary Materials).

 doi:10.20944/preprints202510.0833.v1

3.3. The *waa* Gene

The *waa* gene was specifically amplified by PCR using specific primers designed for this purpose. The amplicons that resulted were sequenced and analyzed. The results obtained showed that it belongs to the *E. coli* O157:H7 strain Sakai, and it was deposited in the NCBI database under accession no. PP059843. Figure 3 (Supplementary Materials) shows the electrophoresis of the *waa* gene obtained by PCR amplification.

3.4. The Shiga Toxin Gene *stx*

Production of Shiga toxin is one of the main characteristics of *E. coli* O157:H7. Our initial survey to identify the type of Shiga toxin showed that it is type 1, which was amplified by PCR and subjected to analysis. The sequence obtained was deposited in NCBI under accession no. OR939814. Figure 4 shows the electrophoresis of the amplified *stx1* gene (Supplementary Materials).

3.5. The *rfbO* Gene

The *rfbO* gene is characteristic for *E. coli* O157:H7. It encodes the O antigen, which is a major component of the bacterium's cell wall. During this study, this gene was targeted for amplification and sequencing, and was found to be similar to that of the *E. coli* O157:H7 strain Sakai. The results of the sequencing were deposited in the NCBI database under accession no. PP059842. Electrophoresis of the amplified *rfb*O gene is shown in Figure 5 (Supplementary Materials).

3.6. Site-Directed Mutagenesis of the *waa* Gene

The *waa* gene was obtained by PCR amplification and was subjected to mutagenesis using a primer specifically designed for this purpose. This primer targeted the sequences on the gene responsible for protein coding, resulting in mutated gene products that encode mutated proteins predicted to be incorporated into the cell wall. The verification of the site-directed mutagenesis of the waa gene is shown in Figure 1.

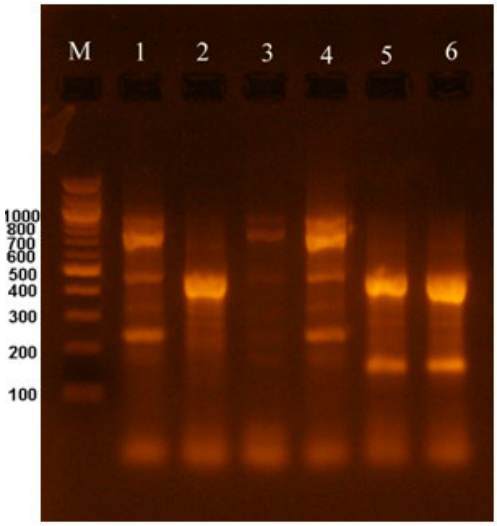

Figure 1. Electrophoresis of the mutated *waa* gene amplified from *E. coli* O157:H7. M is a 100 bp marker DNA. Lanes 1, 2, and 3 represent the mutated *waa* gene from the animal isolate, whereas. Lanes 4, 5, and 6 are the mutated *waa* gene from the human isolate.

3.7. Cloning and Transformation of the Mutated *waa* Gene

The mutated *waa* gene was cloned into the pHTP9 cloning vector. The product of the cloning experiment was used to transform the competent cells and wild-type strains. Positive selection was

 doi:10.20944/preprints202510.0833.v1

the basis on which the transformants were selected since they can resist kanamycin due to the resistant gene harbored by pHTP9. When transformants were able to grow on LB agar supplemented with kanamycin, we performed colony PCR using primers (mutC) and (pH) to target the mutated gene and a specific sequence on pHTP9, respectively. This confirmed the successful transformation procedures. Figure 6 (Supplementary Materials) shows the growth of transformants on kanamycin-supplemented LB medium compared to normal cells, whereas Figure 2 shows the result of the colony PCR.

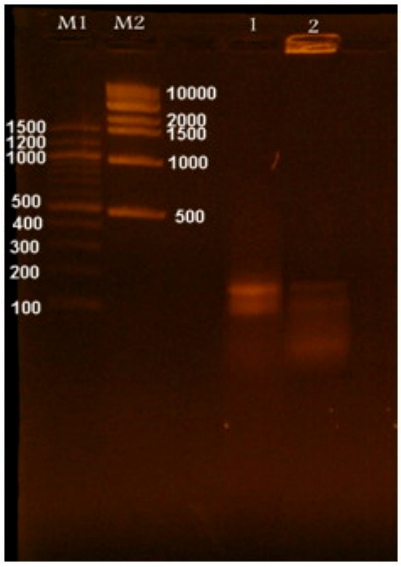

Figure 2. PCR amplification of the mutated gene and pHTP9. M1 is a 500 bp DNA marker, and M2 is a 100 bp DNA marker. Lanes 1 and 2 are the amplification result of the mutated gene and the pHTP9-specific sequence after the cloning experiment and colony PCR, respectively.

3.8. Interpretation of Site-Directed Mutagenesis of the waa Gene

3.8.1. Mutated *waa* K

The *waa* K is responsible for n-acylglucoseamine transferase synthesis, and its product is involved in the modification of the LPS core before attachment to the O antigen. This site was targeted for mutation to investigate the effect of the newly encoded protein on the bacterium. The results are shown in Table 1 (Supplementary Materials).

3.8.2. The *waa* L Gene

The *waa L* gene product is involved in core modification and O antigen coding. A mutation in this gene resulted in specific criteria given in Table 2 (Supplementary Materials).

3.8.3. The *waa* Y Gene

The *waa Y* gene's role is to modify the cell, which increases the size of LPS. Mutation of this gene was performed to study specific characteristics that may be important to cell wall formation. Table 3 (Supplementary materials) gives the changes in this gene's characteristics.

3.8.4. Cell Wall Topology of Mutated E. coli Compared to the Wild Type

In all kinds of bacteria, the cell wall is characterized by a specific topology that enables chemical and biochemical compound exchange and allows for efficient interaction with the environment. Changing the protein structure of the cell wall may result in a change in its topology. In our experiment, the topologies of the cell walls of wild-type *E. coli* and of the mutated type were determined and are summarized in Table 1.

Preprints.org (www.preprints.org) | NOT PEER-REVIEWED | Posted: 13 October 2025 doi:10.20944/preprints202510.0833.v1

Table 1. Topology and characteristics of mutated *E. coli* compared to the wild type.

<table>
<tr><td colspan="2">The 3D structure of mutated waa gene</td><td>Expected biological function</td></tr>
<tr><td colspan="2"> 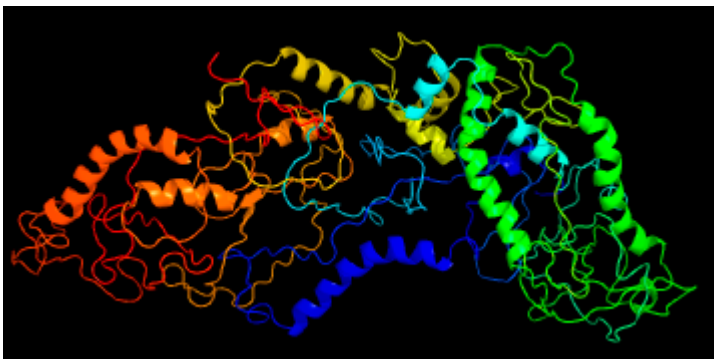
image colored by rainbow N → C terminus
Model dimensions (Å): X:111.214 Y:67.138 Z:102.658</td><td>Putative membrane antigen</td></tr>
<tr><td colspan="3">The secondary structure of mutated waa gene</td></tr>
<tr><td colspan="3"> 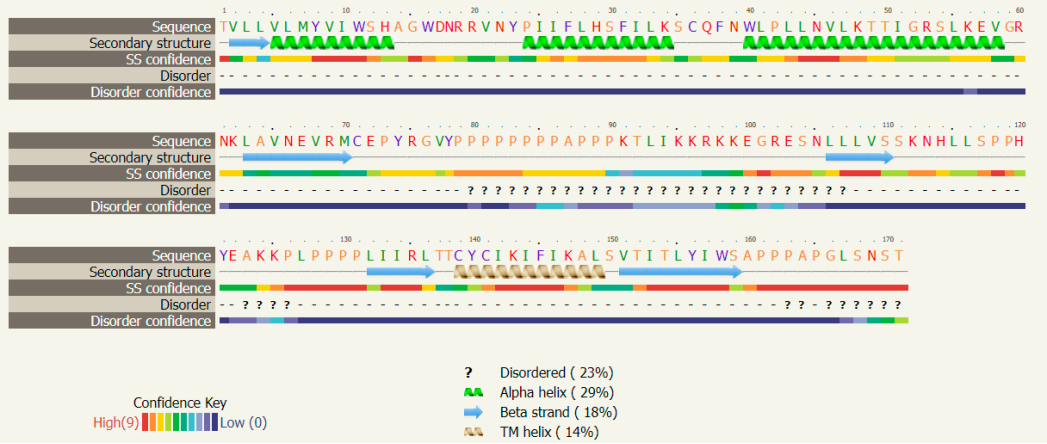
</td></tr>
<tr><td>Function conservation of mutated waa gene</td><td>Conserve amino acid residues in mutated protein</td><td>Position in the sequence</td></tr>
<tr><td></td><td>Uncharacterized</td><td></td></tr>
<tr><td>Mutational sensitivity of mutated waa gene</td><td>Highly sensitive amino acid residues in mutated protein</td><td>Position in the sequence</td></tr>
</table>

 doi:10.20944/preprints202510.0833.v1

	Uncharacterized	
The 3D structure of wild type cell wall		Expected biological function
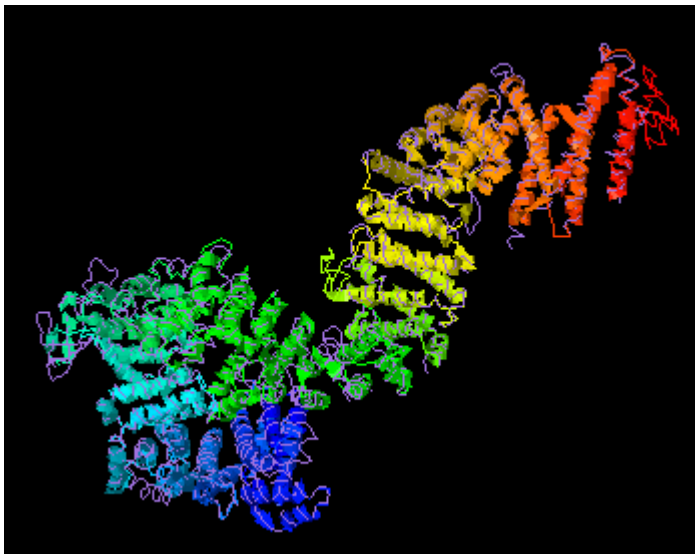 image colored by rainbow N → C terminus Model dimensions (Å): X:47.053 Y:64.719 Z:48.441		Single-Particle Cryo-EM Structure of the *waa* L O-antigen ligase in its ligand bound state, lipopolysaccharide heptosyltransferase-1
The secondary structure of wild type *waa* gene		
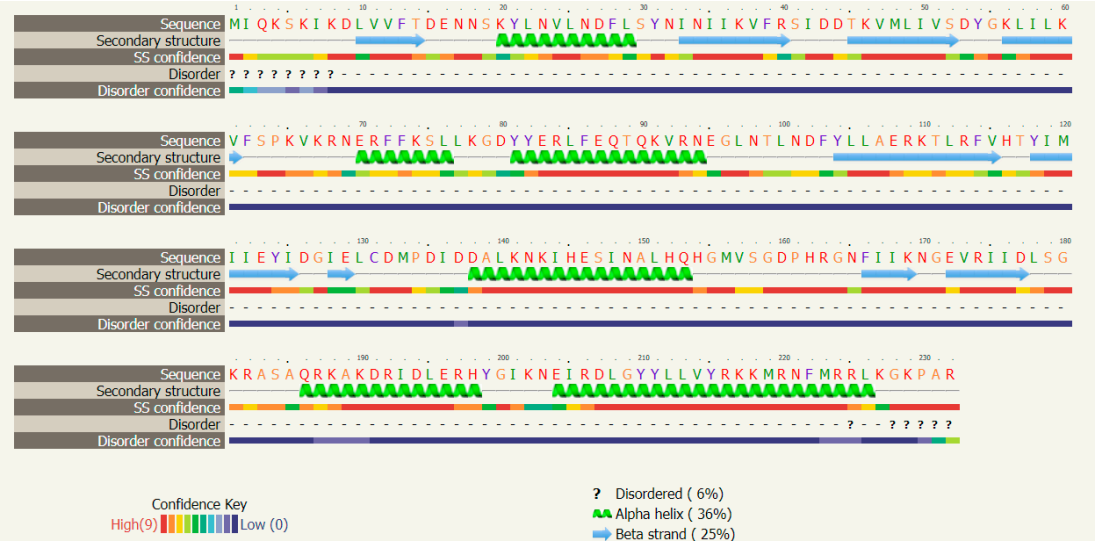		
Function conservation of WILD type *waa* gene	Conserve amino acid residues in wild type protein	Position in the sequence

Preprints.org (www.preprints.org) | NOT PEER-REVIEWED | Posted: 13 October 2025 doi:10.20944/preprints202510.0833.v1

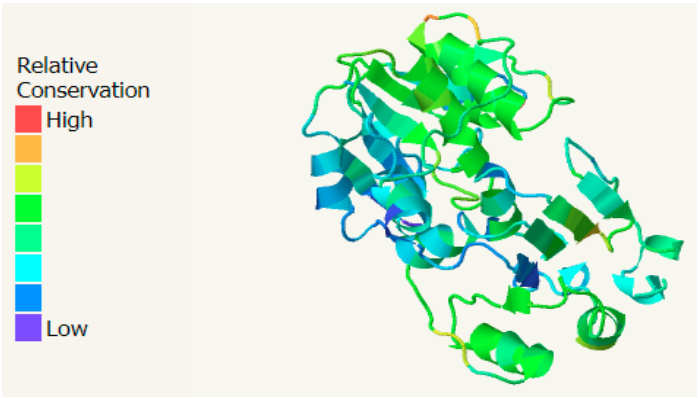	W, Y, Y, Y, P, R, R, Y, P, H, N, Y, H, D, F, D, H, W, E, A, D, P, Y, N, E, Y, Y	88, 106, 137, 152, 218, 265, 288, 292, 303, 380, 239, 368, 466, 529, 565, 706, 711, 737, 889, 951, 970, 999, 1013, 1015, 1039, 1050, 1057
Mutational sensitivity of mutated *waa* gene	Highly sensitive amino acid residues in mutated protein	Position in the sequence
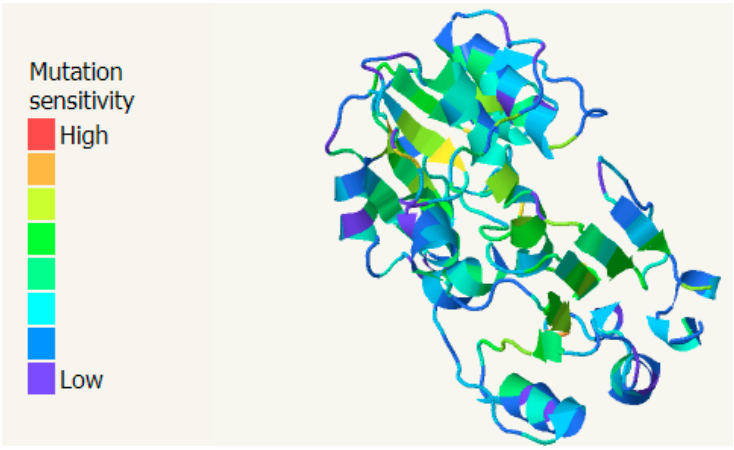	H, W, Y, R, Q, P, R, G, R, Y, P, H, H, N, G, G, K, D, P,	9, 88, 152, 161, 115, 118, 165, 186, 288, 292, 303, 336, 338, 339, 349, 352, 539, 634

Moreover, the transmembrane topologies in both types of bacteria were significantly changed. This can be seen through the arrangement of the spanning proteins integrated in the cell wall and illustrated in Figure 3.

 doi:10.20944/preprints202510.0833.v1

A

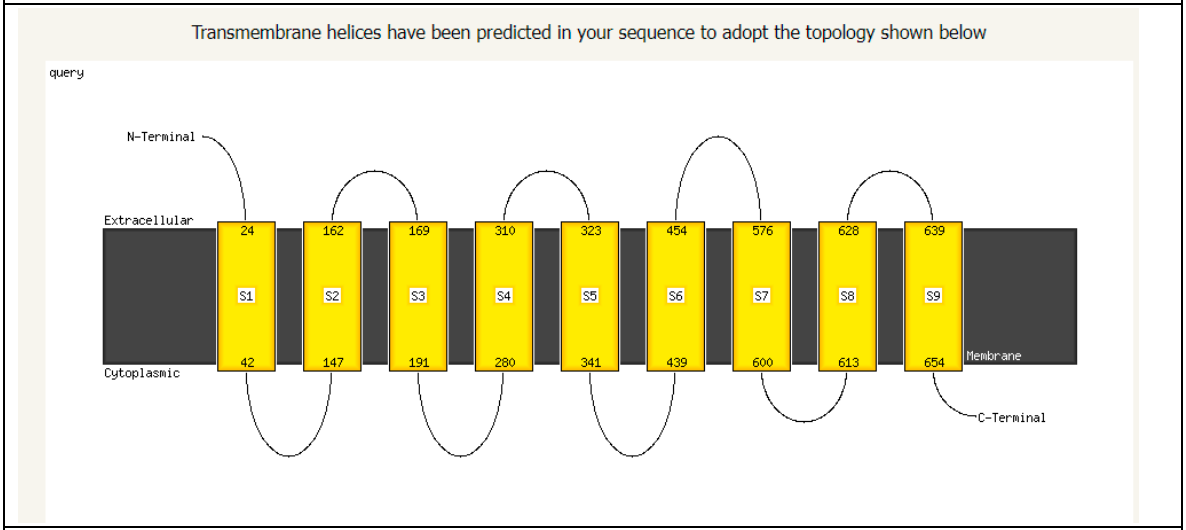

B

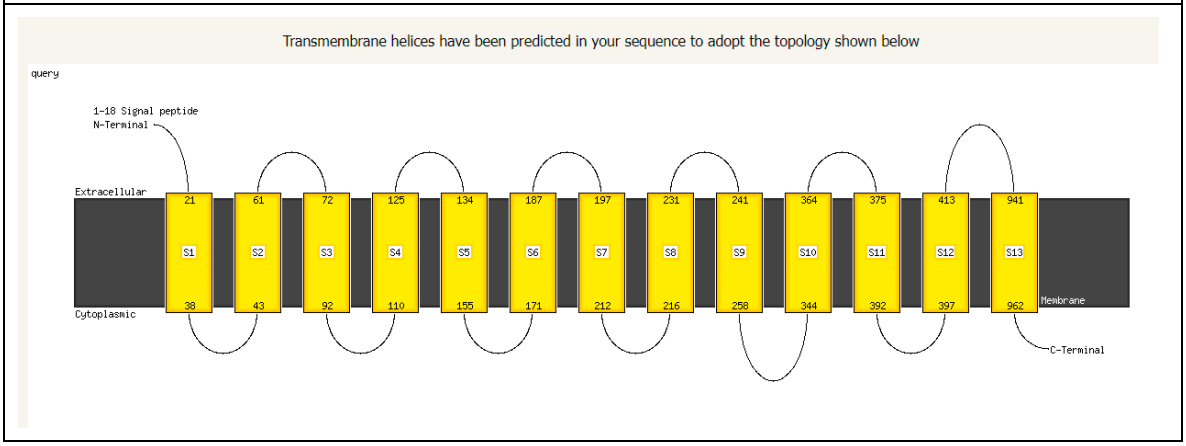

Figure 3. The arrangement of the transmembrane of mutant *E. coli* H7:O157 (A), and wild-type *E. coli* H7:O157 (B). The figure shows a significant change in the spanning proteins in the cell wall.

When applying the Hidden Markov Model (HMM) to both cell walls, significant changes were also predicted and are listed in Table 6 (Supplementary Materials).

In types of cell walls studied and predicted, the distribution of both α / β and TM helices was significantly changed with regard to their location, as well as the A. A. residues involved in this change. These changes are illustrated in Table 8.

Table 8. Changes in type and location of amino acid residues in the mutated and wild-type cell wall of *E. coli* H7:O157.

Mutated cell wall (733 residues)			Wild-type cell wall (1453 residues)		
Location on the cell wall	A.A. sequence	Type of helix	Location of A. A. residue	A.A. sequence	Type of helix
Outside	1-19	α / β	Inside	1-19	α / β

 doi:10.20944/preprints202510.0833.v1

	20-42	TMhelix		20-37	TMhelix
Inside	43-144	α / β	Outside	38-40	α / β
	145-162	TMhelix		41-60	TMhelix
Outside	163-166	α / β	Inside	61-71	α / β
	167-186	TMhelix		72-91	TMhelix
Inside	187-290	α / β	Outside	92-105	α / β
	291-310	TMhelix		106-128	TMhelix
Outside	311-319	α / β	Inside	129-134	α / β
Inside	320-436	α / β		135-157	TMhelix
	437-459	TMhelix	Outside	158-166	α / β
Outside	460-733	α / β		167-189	TMhelix
			Inside	190-195	α / β
				196-213	TMhelix
			Outside	214-239	α / β
				240-259	TMhelix
			Inside	260-345	α / β
				346-368	TMhelix
			Outside	369-371	α / β
				372-394	TMhelix
			Inside	395-398	α / β
				399-418	TMhelix
			Outside	419-1453	α / β

 doi:10.20944/preprints202510.0833.v1

3.9. Laboratory Animal Experiment and Statistical Analysis

3.9.1. Measuring Liver Function in Infected Animals

The laboratory animal study was performed by administering wild- and mutated-type *E. coli* O157:H7 orally to the experimental animals. The animals were observed for infection symptoms and blood was drawn from all animals that showed signs of weakness, diarrhea, and disturbed or weak motion. The liver function of the tested animals was measured and compared with each other, as shown in Table 4 (Supplementary Materials).

3.9.2. Measuring Kidney Function

Infection with *E. coli* O157:H7 can disturb the physiological functioning of the animal. Among the indicators of the infection is the disturbance of kidney function, represented by elevated blood urea and serum creatinine. Measurements of these factors are given in Table 5 (Supplementary Materials).

4. Discussion

Diseases causing diarrhea are considered to be a serious threat to health and well-being. Among these diseases are those caused by *E. coli* [25,26]. *E. coli* O157:H7 can be identified using emerging high-throughput methods such as isothermal DNA amplification, surface-enhanced spectroscopy, biosensors, and rapid paper-based diagnostic methods [27,28].

The lipopolysaccharide (LPS) is the main component of the outer membrane of Gram-negative bacteria, including *E. coli*. It is composed of lipid A, an oligosaccharide core made of glucose, heptose, galactose, 2-keto-3-deoxyoctonate (KDO), and a highly variable component of the O antigen. The location on the chromosome responsible for LPS synthesis is called *waa* , and is composed of three operons. Mutations in *waa* may lead to a truncated LPS with pleotropic effects for bacterial cells, resembling sensitivity to antibiotics and susceptibility to bacteriophages [29].Therefore, studying mutations of the *E. coli* O157:H7 cell wall may provide crucial information about the pathogenicity, infectivity, and severity of the resultant symptoms. The Waa K product is responsible for encoding *N*-acetylglucosamine transferase, and participates in the surface O antigen by facilitating the *N*-acetylglucosamine matrix but it is not absolutely necessary for this purpose [30]. In our study, the wild-type Waa K product was identified as UDP-glycosyltransferase/glycogen phosphorylase, which is the normal function of this location in *the waa* cluster, while in the mutated type, it was identified as a transcription factor, indicating the loss of its identity. Through analysis of this gene, the protein showed an alpha helix from 36% in the wild type to 27% in the mutant, and from 13% to 22% in the beta helix. The interesting finding is that the loss of the transmembrane helix in the mutated gene was measured at 4% in the wild strain.

The function of the mutated gene was totally diminished compared with the wild type, which showed a tendency to lose its function at residues distributed along the gene's DNA sequence. Moreover, the mutational potential in this site seems to be high when tested under the Markov model, starting from amino acid residue 1 and ending with 120, with short intervals between them (Table 1). In an earlier study [31], it seemed that the function of *waa* K is the addition of the α-1,2 terminal to *N*-acetylglucosamine, which forms a branched residue in the outer membrane. Even with a mutated *waa* K, the *N*-acetylglucosamine still has α-1, 2-linked Glc residue at the same position [32]. Thus, it seems that a mutation in this *waa* location does not have high significance in terms of the cell structure, or other biological function, but acts only as a complement to *the waa* L gene [33]. The *waa* L is the only gene known to be required for O antigen ligation during bacterial cell formation [34]. Although considerable information regarding *waa* L has been garnered from in vivo studies, researchers continue to try to understand the role of this gene through mutation studies [35].

In our study, the sequence was identified as a putative cell su*rfa*ce polysaccharide polymerase/ligase of the *waa* L O antigen in the wild type. After mutating this site, the original

 doi:10.20944/preprints202510.0833.v1

function changed to that of a beta-galactosidase enzyme. The alpha helix changed from 72% in the wild type to 23% in the mutant, and the beta helix changed from 0% in the wild type to 20% in the mutant. The significance of this mutation is that the transmembrane helix was reduced from 52% in the wild type to 12% in the mutant version of the bacterium. Consequently, such a change led to the low function preservation represented by most amino acid residues along the encoded protein. The mutational hot spots changed when the two types of bacteria were compared (Table 2).

The *waa* L mutant is unable to cap the lipid A-core with relaxed specificity for the polymer, to which it attaches, and it is essential for O antigen transfer to the cell; it significantly contributes to cell wall topology [36]. Previous reports showed that, if the *waa* L loses its function, it will result in a full-length core OS that is not capped by O-PS [37]. The *waa* Y product is part of *the waa* P gene responsible for the phosphorylation activity during cell wall formation. The *waa* Y product is located in the central part of the *waa* operon and is involved in the assembly of the core region of the LPS molecule. The loss of this gene activity resulted in the loss of phosphoryl substituents [38]. In this study, we investigated the effect of mutation on the function of *waa*Y. There was a significant shift in this gene function. Instead of performing kinase activity on the heptose molecule, it shifts to transferase activity (Table 3 supplementary materials). This can be explained by forming transmembrane helices in the mutant type that was not detected in the wild type, which reached 14% of the secondary structure of the protein. Furthermore, both the alpha and beta helices in the wild type changed from 36% and 25% to 29% and 18%, respectively. The mutation susceptibility was found to be very low in the wild type and limited to the G, F, and H residues located at 127, 178, and 198 of the protein. Instead, this characteristic increased in the mutated protein. From our study, it seems that the *waa* Y gene is a highly preserved location due to its low susceptibility to genetic change, with the essential function of LPS phosphorylation as previously reported [39,40].

4.1. Cell Wall Topology

In this study, the site-directed mutagenesis inflicted on multiple essential *waa* sites may facilitate the prediction of a form of cell wall topology that *E. coli* H7:O157 can obtain. We found that, in spite of multiple mutations in the *waa* operon, the bacterium still keeps the O antigen characteristic on its surface, suggesting that even with the *waa* L mutation, the cell possesses an alternative mechanism to include this protein. The interesting observation we found when the whole surface LPS of mutated-type *E. coli* H7:O157 after reconstruction (Table 4 Supplementary Materials) showed that there was a change in the secondary structure helices to form a transmembrane type, resulting in a decrease of about 14% compared to the wild type. We were unable to determine the function preservation and mutational hot spots in the mutated type, while in the wild type; function preservation was moderate with a low tendency to mutation as given in figure 3.

4.2. Effect of Mutation on E. coli O157:H7 Infectivity and Pathogenicity

There are certain *E. coli* isolates associated with diseases in humans and animals worldwide [41] with different virulence strategies [42,43]. Studies have shown that *E. coli* pathogenicity may be attributed to the harboring of genes that resist antimicrobial agents, the formation of biofilm [44], or the production of toxins such as α-hemolysin [45] and cytotoxic necrotizing factor 1 [46]. In our experiment, laboratory animals were exposed to both wild-type and mutated *E. coli* H7:O157 to determine the effect of cell wall mutation on this bacterium's pathogenicity and morbidity. We found that the mice exposed to the mutant *E. coli* H7:O157 showed infection symptoms within about 24 hours, and half of them died within 6 hours of infection symptoms appearing. When compared to the group infected with wild-type *E. coli* H7:O157, the time of morbidity and mortality doubled. This can be explained by the significant release of Shiga toxin that destroyed the intestines of the mice and spread through their blood, causing a significant elevation in liver and kidney enzymes, as illustrated in Tables 7 and 8. Thus, infection with mutant *E. coli* H7:O157 caused direct hemolytic uremic syndrome (HUS) [47,48]. In normal cases of infection with EHEC, the toxin is released as a free protein liberated from the periplasmic space or enclosed in the outer membrane, ready to be released by

 doi:10.20944/preprints202510.0833.v1

Gram-negative bacteria [49]. In our case of the mutated bacterium, the cell wall structure is significantly changed, which might eventually lead to the uncontrolled release of the Shiga toxin into the lab animals' intestines or may be retained in the outer membrane ready to release on demand, which is why we expected a lack of Shiga toxin cluster formation [50]. The limitation in this study is that the *waa* operon contains other genes that it may inflect their effect on the pathology of the bacterium that we couldn't study here. We recommend that these genes effect to be studied in antibiotic resistance and the ability of *E. coli* H7:O157 ability to infect their hosts.

5. Conclusions

E. coli H7:O157 is highly abundant in foods exposed to infected animal feces and foods derived from animal products. It is the main cause of many outbreaks and severe infections that may be life-threatening. It is characterized by the production of Shiga toxins, which inflict damage to the small intestine, which the bacterium colonizes, and which is considered the main virulence factor. Another virulence factor in this bacterium is its tendency to resist antibacterial agents, which is known to be a progressive trait. The main control system in these cases is the cell wall through which material exchange takes place. When the cell is subjected to change, the bacterium becomes more aggressive, and the production of Shiga toxin increases dramatically. Our investigation showed the modification of the cell wall topology, which happened on a molecular level when one or more genes comprising the *waa* operon were changed. *waa* L and *waa* K were found to be the most effective sites that can play this role. This may provide insight that would be useful in the design of new drugs to counter *E. coli* H7:O157 infection in a way that does not invoke cell wall modification that may result in more aggressive strains of the bacterium.

Supplementary Materials: The following supporting information can be downloaded at the website of this paper posted on Preprints.org.

Author Contributions: Walla A. Salloomi performed sample collection, DNA extraction, and PCR amplification; Rebah N. Algafari performed data analysis and article drafting; and Ikram Abbas Abbood supervised the progress of the project.

Funding: Not applicable.

Institutional Review Board Statement: This study was approved by the College of Veterinary Medicine IRB and animal welfare committee and was issued with approval no. PG/244.

Informed Consent Statement: All authors approved the publication of the article after reviewing the results, discussion, and draft.

Data Availability Statement: The data recorded, samples collected, questionnaires, and genomic DNA, and PCR products used during this study are available and stored at https://zenodo.org/uploads/14623186 with DOI: 10.5281/zenodo.14623186.

Acknowledgments: Not applicable.

Conflicts of Interest: This research was conducted without any competing interests among the authors or with any other research group at other institutions.

References

1. Fontaine R, Arnon S, Martin W. Raw hamburger: An interstate common source of human salmonellosis. Am J Epidemiol. 1978, 107(1):36-45. doi: 10.1093/oxfordjournals.aje.a1125051978
2. Blanco M, Blanco J, Mora A, Dahbi G, Alonso M, González E. Serotypes, virulence genes, and intimin types of Shiga toxin (verotoxin)-producing Escherichia coli isolates from cattle in Spain and identification of a new intimin variant gene (eae-xi). J Clin Microbiol. 2004, p. 645–651
3. Al-Khyat F. Enterohaemorrhagic *E. coli* O157 in locally produced soft cheese. Iraqi J. Vet. Med. 2008, 32 (1); 88-99.

 doi:10.20944/preprints202510.0833.v1

4. Guth B, Prado V, Rivas M. Shiga toxin-producing Escherichia coli. In: Torres AG, editor. Pathogenic Escherichia coli in Latin America. Galveston, TX, USA: Department of Microbiology and Immunology, Sealy Institute for Vaccine Sciences, University of Texas Medical Branch; 2010
5. Paton AW, Paton JC. Direct detection of Shiga toxigenic Escherichia coli strains belonging to serogroups O111, O157, and O113 by multiplex PCR. J Clin Microbiol. 1999; 37:3362–3365.
6. Heiman KE, Mody RK, Johnson SD, Griffin PM, Gould LH. Escherichia coli O157 outbreaks in the United States, 2003–2012. Emerg Infect Dis. 2015;21(8). doi:10.3201/eid2108.141364.
7. Ahmed S. T., Jasim A.N., Ali A. M. Isolation and characterization E. coli O157:H7 from meat and cheese and detection of Stx1, Stx2, hlyA, eaeA using multiplex PCR. 2011. JOBRC. 5(2) p: 15-24.
8. Van TTH, Yidana Z, Smooker PM, Coloe PJ. Antibiotic use in food animals worldwide, with a focus on Africa: pluses and minuses. J Glob Antimicrob Resist. 2020; 20:170–177. doi:10.1016/j.jgar.2019.07.031.
9. Mohammed Z. A. Isolation and Identification of *Escherichia coli* O157:H7 from locally minced meat and imported minced and chicken meat. Iraqi J. Vet. Med. 2008, 32(1); 100-113.
10. Hasan J. M., Najim S. S. A review of the Prevalence of Enterohemorrhagic E. coli in Iraq. 2024. JOBRC. 18 (1) p: 33-39
11. Khalil Z. K. Isolation and identification of Staphylococcus aureus, Listeria monocytogenes, E. coli O157:H7 and Salmonella specious from raw beef and lamb meat in Baghdad by PCR. Iraqi Journal of Science, 2016, 57 (3B), 1891-1897.
12. Lim JM, Singh SR, Duong MC, Legido-Quigley H, Hsu LY, Tam CC. Impact of national interventions to promote responsible antibiotic use: a systematic review. J Antimicrob Chemother. 2020;75(1):14–29. doi:10.1093/jac/dkz348
13. Nataro JP, Kaper JB. Diarrheagenic Escherichia coli. Clin Microbiol Rev. 1998;11(1):142–201. doi:10.1128/CMR.11.1.142 37. Caprioli A, Morabito S, Brugere H, Oswald E. Enterohaemorrhagic Escherichia coli: emerging issues on virulence and modes of transmission. Vet Res. 2005;36(3):289–311. doi:10.1051/vetres:2005002.
14. Beata S, Michał T, Mateusz O, et al. Norepinephrine affects the interaction of adherent-invasive Escherichia coli with intestinal epithelial cells. Virulence. 2021; 12:630–637. doi:10.1080/21505594.2021.1882780.
15. Thompson JS, Hodge DS, Borczyk AA. Rapid biochemical test to identify verocytotoxin-positive strains of Escherichia coli serotype O157. J Clin Microbiol. 1990; 28:2165–2168.
16. Perna NT, Plunkett G, Burland V, Mau B, Glasner JD, Rose DJ, et al. Genome sequence of enterohaemorrhagic Escherichia coli O157:H7. Nature. 2001;409:529–533.
17. Dobrindt U, Agerer F, Michaelis K, Janka A, Buchrieser C, Samuelson M, et al. Analysis of genome plasticity in pathogenic and commensal Escherichia coli isolates by use of DNA arrays. J Bacteriol. 2003;185:1831–1840.
18. Wick LM, Qi W, Lacher DW, Whittam TS. Evolution of genomic content in the stepwise emergence of Escherichia coli O157:H7. J Bacteriol. 2005;187:1783–1791.
19. Amézquita-López BA, Quiñones B, Soto-Beltrán M, et al. Antimicrobial resistance profiles of Shiga toxin-producing Escherichia coli O157 and non-O157 recovered from domestic farm animals in rural communities in Northwestern Mexico. Antimicrob Resist Infect Control. 2016;5(1):1. doi:10.1186/s13756-015-0100-5.
20. Aklilu, F., Daniel, K., & Ashenaf, K. (2017). Prevalence and antibiogram of Escherichia coli O157 isolated from bovine in Jimma, Ethiopia: Abattoir-based survey. Ethiopian Veterinary Journal, 21(2), 109–120.
21. Aschalew Ayisheshim Tarekegn, Birhan Agimas Mitiku, Yeshwas Ferede Alemu. Escherichia coli O157:H7 beef carcass contamination and its antibiotic resistance in Awi Zone, Northwest Ethiopia. 2023, Food Sci Nutr. 2023;11:6140–6150.
22. Gambushe S. M., Zishiri O., Zowalaty M. E El. Review of Escherichia coli O157:H7 Prevalence, Pathogenicity, Heavy Metal and Antimicrobial Resistance, African Perspective. Infection and Drug Resistance, 2022:15 4645–4673.
23. Banerjee S, Lo K, Ojkic N, Stephens R, Scherer NF, Dinner AR. 2021. Mechanical feedback promotes bacterial adaptation to antibiotics. *Nat Phys* 17:403–409.
24. Harris LK, Theriot JA. 2016. Relative rates of surface and volume synthesis set bacterial cell size. *Cell* 165:1479–1492.

 doi:10.20944/preprints202510.0833.v1

25. Ojkic N, Banerjee S. 2021. Bacterial cell shape control by nutrient-dependent synthesis of cell division inhibitors. *Biophys J* 120:2079–2084.
26. Nikola Ojkica, Diana Serbanescua, Shiladitya Banerjee. Antibiotic Resistance via Bacterial Cell Shape-Shifting. ASM, May/June 2022 Volume 13 Issue 3 e00659-22. https://doi.org/10.1128/mbio.00659-22
27. Nikolic P. and Mudgil P. The Cell Wall, Cell Membrane and Virulence Factors of Staphylococcus aureus and Their Role in Antibiotic Resistance. Microorganisms 2023, 11(2), 259; https://doi.org/10.3390/microorganisms11020259
28. WHO estimates of the global burden of foodborne diseases: foodborne disease burden epidemiology reference group 2007–2015
29. Sndra B. March and Samuel R. Sorbitol-MacConkey Medium for Detection of Escherichia coli 0157:H7 Associated with Hemorrhagic Colitis. JOURNAL OF CLINICAL MICROBIOLOGY, 1986, p. 869-872.
30. Dagny Jayne Leininger, Jerry Russel Roberson, Franc¸ois Elvinger. Use of eosin methylene blue agar to differentiate Escherichia coli from other gram-negative mastitis pathogens. J Vet Diagn Invest 13:273–275 (2001).
31. Ally C. Antony, Mini K. Paul, Reshma Silvester, Aneesa P.A., Suresh K., Divya P.S., Simmy Paul, Fathima P.A. and Mohamed Hatha Abdulla. Comparative Evaluation of EMB Agar and Hicrome E. coli Agar for Differentiation of Green Metallic Sheen Producing Non-E. coli and Typical E. coli Colonies from Food and Environmental SamplesJ. Pure.App. Microbiol. 2016, 10,4 p. 2863-2870.
32. Rani A., Ravindran V. B., Surapaneni A., Mantri N., Ball A. S. Review: Trends in point-of-care diagnosis for Escherichia coli O157:H7 in food and water. International Journal of Food Microbiology, 349, 2 2021, 109233
33. Pagnout C., Sohm B., Razafitianamaharavo A., Caillet C., Offroy M., Leduc M., Gendre H., Jomini S., Beaussart A., Bauda P., Duval J. F L Pleiotropic effects of rfa-gene mutations on Escherichia coli envelope properties. Sci Rep. 2019; 4;9:9696. doi: 10.1038/s41598-019-46100-3
34. Raetz, C.R. · Whitfield, C. Lipopolysaccharide endotoxins Annu. Rev. Biochem. 2002; 71:635-700
35. Han W., Wu B., Li L., Zhao G., Woodward R., Pettit N., Cai L., Thon V., Wang P. Defining Function of Lipopolysaccharide O-antigen Ligase WaaL Using Chemoenzymatically Synthesized Substrates. Microbiology. 2012; 287(8),5357-5365.
36. Abeyrathne P. D, Daniels C., Poon K. K H, Matewish M. J, 1, Craig Daniels 1,†, Karen K H Poon 1, Matewish M. J, Lam J. S. Functional Characterization of WaaL, a Ligase Associated with Linking O-Antigen Polysaccharide to the Core of Pseudomonas aeruginosa Lipopolysaccharide. J Bacteriol. 2005;187(9):3002–3012. doi: 10.1128/JB.187.9.3002-3012.2005.
37. Klena, J. D., Ashford, R. S., II, and Schnaitman, C. A. (1992) J. Bacteriol. 174; 7297-7307.
38. Kaniuk, N. A., M. A. Monteiro, C. T. Parker, and C. Whitfield. Molecular diversity of the genetic loci responsible for lipopolysaccharide core oligosaccharide assembly within the genus Salmonella. Mol. Microbiol. 2002; 46:1305-1318.
39. Frirdich E., Lindner B., Holst O., Whitfield C. Overexpression of the waaZ Gene Leads to Modification of the Structure of the Inner Core Region of Escherichia coli Lipopolysaccharide, Truncation of the Outer Core, and Reduction of the Amount of O Polysaccharide on the Cell Surface. J Bacteriol. 2003; 185(5):1659–1671. doi: 10.1128/JB.185.5.1659-1671.2003
40. Yethon J. A., Heinrichs D., Monteiro M. A., Perry M. B., Whitfield C. Involvement of waaY, waaQ, and waaP in the Modification of Escherichia coli Lipopolysaccharide and Their Role in the Formation of a Stable Outer Membrane. J. Biol. Chem. 1998; 273(41), 26310-26316
41. Taylor C. M, Goldrick M., Lord L., Roberts I. S . Mutations in the waaR Gene of Escherichia coli Which Disrupt Lipopolysaccharide Outer Core Biosynthesis Affect Cell Surface Retention of Group 2 Capsular Polysaccharides. J Bacteriol. 2006; 188(3):1165–1168. doi: 10.1128/JB.188.3.1165-1168.2006
42. Al wendawi SH. A., Al Rekaby S.M. THE EFFECIENCY OF ENTERIC LACTOBACILLUS IN PREVENTING HEMORRHAGIC COLITIS AND BLOCKING SHIGA TOXINS PRODUCTIONS IN RATS MODELS INFECTED WITH ENTEROHEMORRHAGIC ESCHERICHIA COLI (EHEC). Iraqi Journal of Agricultural Sciences.2021; 52(6):1346-1355.
43. Al-Taii D. H. F. Effects of *E. coli* O157:H7 Experimental Infections on Rabbits. Iraqi J. Vet. Med. 2019; 43 (1), 34-42
44. Wang J., Ma W., Wang X. Insights into the structure of Escherichia coli outer membrane as the target for engineering microbial cell factories. Microb Cell Fact. 2021; 20:73 https://doi.org/10.1186/s12934-021-01565-8

 doi:10.20944/preprints202510.0833.v1

45. Kaper, J. B., Nataro, J. P. & Mobley, H. L. Pathogenic Escherichia coli. Nature Rev. Microbiol. 2004; 2, 123–140.
46. Croxen M. A. and Finlay B. B. Molecular mechanisms of Escherichia coli pathogenicity. Nature Reviews Microbiology. 2010; 8, 26–38
47. Sora V. M., Meroni G., Martino P. A., Soggiu A., Bonizzi L. and, Zecconi A. Extraintestinal Pathogenic Escherichia coli: Virulence Factors and Antibiotic Resistance. Pathogens 2021, 10(11), 1355; https://doi.org/10.3390/pathogens10111355
48. Abdul khaleq M. A., Abd A.H., Dhahi M. A. Efficacy of Combination of Meropenem with Gentamicin, and Amikacin against Resistant E. coli Isolated from Patients with UTIs: in vitro Study. Iraqi J Pharm Sci; 2011, 20 (2), 66-74
49. Khan Md F., Rashid S. S. Molecular Characterization of Plasmid-Mediated Non-O157 Verotoxigenic Escherichia coli Isolated from Infants and Children with Diarrhea. Baghdad Science Journal. 2020, 17(3):710-719
50. Wang X., Yu D., Chui L., Zhou T., Feng Y., Cao Y. and Zhi S. A Comprehensive Review on Shiga Toxin Subtypes and Their Niche-Related Distribution Characteristics in Shiga-Toxin-Producing E. coli and Other Bacterial Hosts. Microorganisms 2024, 12(4), 687; https://doi.org/10.3390/microorganisms12040687